Int. J. Heat Mass Transfer. Vol. 30, No. 12, pp. 2549–2557, 1987
Printed in Great Britain

0017–9310/87 $3.00+0.00
Pergamon Journals Ltd.

Heat transfer in the post dryout region and on wetting heated surfaces

N. G. RASSOKHIN and L. P. KABANOV
Moscow Power Engineering Institute, Moscow, U.S.S.R.

(*Received* 20 *May* 1985 *and in final form* 8 *August* 1986)

Abstract—A survey is given of the works published in the Soviet Union during 1983 and 1984 on heat transfer in the post dryout region and on wetting heated surfaces. New experimental data, heat transfer models, and computational techniques are analysed. The complexities of the heat transfer process under the above conditions are noted. The differences and common features of the heat transfer processes in the post dryout region and on wetting heated surfaces are indicated as well as the necessity for the development of computational techniques that would consider the two processes simultaneously.

1. INTRODUCTION

DURING 1983 and 1984 new publications appeared in the Soviet Union on heat transfer in the post dryout region and on wetting heated surfaces under different conditions as regards the operational parameters, characteristics of test sections and supply of cooling water. Investigations were carried out both to reveal and refine separate experimental characteristics of the heat transfer process and to further develop heat transfer models and computational techniques for application to different conditions and regions of flow.

A number of earlier works [1–5] surveyed foreign and home investigations into the post dryout heat transfer and heat transfer on wetting heated surfaces. The present review continues the analysis of novel experimental data, empirical correlations and computational models under the above-mentioned conditions. Experimental data are cited which were obtained in channels of different geometries in the cases of reduced flow rates and relatively small pressures of two-phase flows, further development of heat transfer models for vapour–droplet flow is outlined, interrelation between the modes of steady-state post dryout heat transfer and wetting of heated surfaces is established.

2. CRITICAL VAPOUR QUALITY AND POST DRYOUT HEAT TRANSFER

A detailed analysis of the onset of burnout heat transfer during water boiling in tubes is presented in ref. [6]. This work gives the current ideas of the mechanisms underlying the dryout phenomenon in vapour-generating channels, analyses the specific features of dryouts in the case of non-uniform heat generations along the channel length and presents the data on the limiting vapour quality. Special emphasis is placed on the necessity for distinguishing between the mass vapour qualities x_{lim} and x^0_{lim} at which the dryout heat transfer of the second kind develops depending on the vapour quality at the channel entrance. When $x_{\text{en}} > x_{\Delta p}$, the value of x_{lim}, at which the dryout heat transfer sets in, is generally higher than x^0_{lim} which corresponds to the dryout heat transfer when $x_{\text{en}} < x_{\Delta p}$. This work also presents the earlier published recommendations for the calculation of x_{lim} and x^0_{lim}.

Based on the analysis of the conditions for the liquid entrainment from the film surface in an annular dispersed flow, in ref. [7] the following empirical formula is suggested to calculate the limiting vapour quality:

$$x^0_{\text{lim}} = 1 - 0.86 \exp(-19/\omega) \qquad (1)$$

where

$$\omega = \rho w \sqrt{\left(\frac{D}{\delta \rho'}\right)}.$$

Comparison is made between the experimental data on the limiting vapour qualities for water flow in circular tubes with the results calculated by equation (1). The majority of points deviate from equation (1) by no more than 20%, with the r.m.s. deviation of 0.12 and mean deviation of 0.035. The same deviation is also observed for three other liquids: Freon-12, Freon-113 and He-1. The data for water encompasses 184 points obtained at: $P = 3$–16.7 MPa, $\rho w = 55$–5000 kg m^{-2} s^{-1}, $D = 3.84$–30 mm.

In ref. [8], based on the local hypothesis about the dryout heat transfer, a formula is suggested for calculating the vapour quality at the time of dryout heat transfer occurrence at reduced ρw. The specific feature of the formula is the use, on the basis of the regression analysis, of similarity numbers taking into account the physical processes that lead to the dryout heat transfer in annular dispersed flow.

In ref. [9] the results of an experimental and computational investigation into the non-equilibrium two-phase flow in the post dryout boiling region at small mass velocities and low pressure are given. The

NOMENCLATURE

a	thermal diffusivity [$m^2 s^{-1}$]
c_p	heat capacity [$kJ kg^{-1} K^{-1}$]
D, d	diameter [m]
G	flow rate [$kg s^{-1}$]
L, l	length [m]
Nu	Nusselt number
P, p	pressure [MPa]
Pr	Prandtl number
Q, q	heat flux [$W m^{-2}$]
r	latent heat of evaporation [$kJ kg^{-1}$]
Re	Reynolds number
S	slip
T	temperature [°C]
ΔT	temperature difference [°C]
T_q	characteristic wetting temperature [°C]
x	vapour quality
$x_{\Delta p}$	vapour quality in the course of microfilm formation
z	coordinate [m].

Greek symbols

α	heat transfer coefficient [$kW m^{-2} K^{-1}$]
δ	droplet diameter [m]
δ_*	vapour layer thickness
λ	thermal conductivity [$W m^{-1} K^{-1}$]
μ	dynamic viscosity [Pa s]
ρ	void fraction; density [$kg m^{-3}$]
ρw	mass velocity [$kg m^{-2} s^{-1}$]
σ	surface tension [nm^{-1}]
τ	time [s].

Subscripts

a	actual
cr	critical
e	equilibrium
ex	exit
fr	wetting front
in	inlet
l	liquid
lim	limiting
s	saturation
v	vapour
w	wall
wet	wetting.

Superscripts

$'$	water at saturation
$''$	vapour at saturation.

experiments were carried out in a rectangular channel with heating on one side. The channel was 0.035 m wide, 0.72 m long and 0.008 m high. The heater was a nichrome plate 0.372 m long. The wall temperature was measured at 25 cross-sections along the channel length by chromel–alumel thermocouples. In the opposite, thermally insulated, wall there were seven static pressure taps and holes for the probes to measure the vapour phase temperature profile and the degree of dispersiveness of droplets. The thermal probe operates on the principle of liquid separation from a two-phase mixture being sucked through a slit between the outer tube and the inner hood. The experiments were run at mass velocities $\rho w = 16.9$, 33.8, 67.6, and 168.9 kg m^{-2} s^{-1}; at a pressure of $P = 0.1$ MPa, a vapour quality $x = 0.75$–0.98 and heat fluxes of 5.0–450.9 kW m^{-2}.

The thermal probe measured vapour temperature profiles in the gap between the heated and non-heated surfaces of the channel which were then used to calculate the thermal non-equilibrium state of the flow and the true vapour quality of the flow was calculated.

The results of all the experiments have been processed and an empirical formula has been suggested which is a refined version of that suggested earlier [10]

$$\frac{x_a}{x_e} = \frac{x_{in}}{x_e} + [9.04(x_{in})^{-1.97}(\rho w/300)^{0.76(x_{in})^{-0.33}}] \times (1 - x_{in})(x_e - x_{in}).$$

In ref. [11] the length of the transient zone of the post dryout heat transfer in a channel of complex geometry (Fig. 1) was determined experimentally. The channel cross-section simulates a cell formed by four tubes. This shape of the channel leads to its higher total thermal loading and, correspondingly, to more stringent heat transfer conditions as compared with real ones. The hydraulic diameter of the channel was 5.6 mm and its length was 1.8 m. The test section was equipped with 50 chromel–alumel thermocouples with electrodes 0.2 mm in diameter welded at 27 cross-sections over the channel height (1–6 thermocouples in each). The interrogation of the probes in the course of the experiment and the management of the rig were made with the aid of a Hewlett–Packard HP-305 2A measuring-computational complex. The wall temperature measurements around the channel perimeter showed that the crisis starts to develop in its narrow portion. Therefore, the results are discussed which were obtained when measuring the wall temperature on the generatrices 'a' and 'b' (Fig. 1).

The paper presents the data on the characteristics of the transient zone, post dryout heat transfer, vapour superheating in the case of upward water flow within the ranges: $3.1 < P < 7.28$ MPa, $30 < \rho w < 455$ kg m^{-2} s^{-1}, $71 < q < 960$ kW m^{-2}.

The analysis has shown that the transient zone length l depends on q and ρw. The quantity l increases with q; at constant q an increase of ρw leads to a decrease of l (Fig. 2).

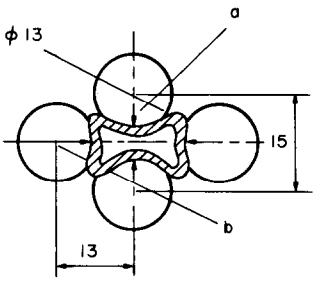

FIG. 1. Schematic of a channel of complex geometry [12].

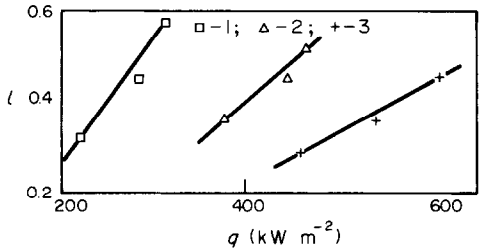

FIG. 2. The length of the transient zone [12]: $P = 7$ MPa; 1, $\rho w = 240$; 2, 340; 3, 440 kg m^{-2} s^{-1}.

The true vapour temperature was determined by continuously recording the flow temperature T_v before and after the separator, which was installed at the channel exit to separate the liquid and vapour phases. The flow temperature was determined with the aid of thermocouples made from a thermocouple cable 0.5 mm in diameter. The maximum value of T_v was taken to be the superheated vapour temperature T_{sv}. Figure 3 presents the dependence of T_{sv} on the overall heat Q provided a saturated liquid was supplied to the channel entrance. It is found that the vapour superheat $T_{sv} - T_s$ increases with Q, while its maximum value reaches 255°C. An increase of ρw leads to a decrease of the vapour superheat and to a decrease in the slope of the curves $T_{sv}(Q)$. A preliminary analysis shows that T_{sv} is qualitatively described by the formula for x_a [10] derived on the basis of the two-stage heat transfer model.

In ref. [12] an investigation is made of heat transfer deterioration in the case of upward and downward water flows in a uniformly heated circular stainless steel tube with an inner diameter of 10 mm and a length of 6.2 m. Ninety experiments were carried out at a pressure of 13.7 MPa, mass velocities $\rho w = 350$–1000 kg m^{-2} s^{-1}, $q = 130$–450 kW m^{-2}, $x_{ex} = 0.4$–1.38. Subcooled water was supplied to the entrance. Chromel–coppel thermocouples were located 100 mm apart.

To directly compare the experimental data and reveal the effect of flow direction on the heat transfer deterioration in the cases of downward and upward flows, the experiments were carried out at the same magnitude of power, flow rate and water temperatures at the test section entrance, with the experiments being first conducted with the downward and with the upward flow.

The tube inner surface temperature in downward flow can be both higher and lower than the wall temperature in upward flow. There is a single-valued relationship between the temperature conditions and the critical vapour quality x_{cr} determined by the discontinuity of the temperature curves: the smaller x_{cr}, the higher T_w, other conditions being equal. When x_{cr}s for the downward and upward flow coincide, the temperature conditions in the post dryout region also coincide. This coupling is attributed by the authors to the fact that the post dryout heat transfer is determined not only by the local conditions, but also by the conditions of two-phase flow formation over the entire preceding section including that of the dryout heat transfer. The conditions in the latter section depend in a complex manner on the operational parameters and flow direction.

The analysis of surface temperature distributions along the section length provided the data on the maximum wall superheats in the post dryout region. The maximum superheat was taken to be the value $\Delta T_{max} = T_{max} - T_s$, where T_{max} is the maximum wall temperature. The following formulae were obtained to determine ΔT_{max}: $\Delta T_{max} = 0.41q/\rho w$ for an upward flow and $\Delta T_{max} = 4.1 \times 10^{-5} q^{1.8}/(\rho w)^{1.1}$ for a downward flow.

The accuracy of experimental data description at $\rho w = 500$–1000 kg m^{-2} s^{-1} and $q = 260$–400 kW m^{-2} amounted to $\pm 8\%$ for upward flow and $\pm 5\%$ for downward flow.

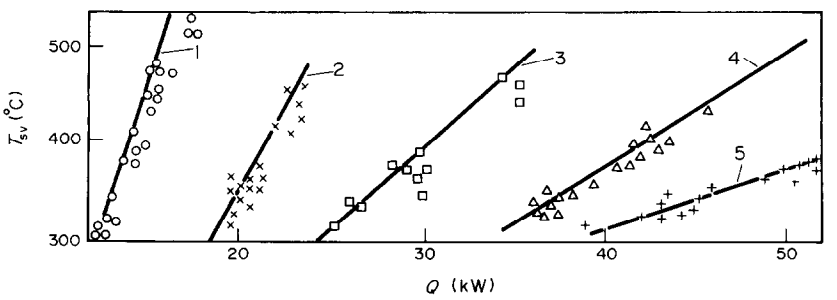

FIG. 3. Temperature of the superheated steam [12] T_{sv} as a function of the heat supplied Q: $P = 7$ MPa; $T_s = 285$°C; 1, $\rho w = 100$; 2, 160; 3, 240; 4, 360; 5, 440 kg m^{-2} s^{-1}.

3. MODELS OF POST DRYOUT HEAT TRANSFER AND CALCULATIONAL RECOMMENDATIONS

In ref. [13] a technique was developed for the calculation of heat transfer to a dispersed steam–water flow over the post dryout section of a steam generating channel. The results of numerical calculations have shown that the presence of liquid droplets colliding with the wall changes the processes of momentum and heat transfer in steam flow.

Two components of heat removal from the wall were considered

$$Q = Q_{wv} + Q_{w\delta}$$

where Q_{wv} is the heat withdrawn by the steam component of a two-phase flow; $Q_{w\delta}$ is the heat transferred from the wall to droplets directly contacting with it.

To calculate the heat flux from a wall to vapour, the familiar empirical relation was used for a one-phase flow with a correction for the presence of the initial thermal portion in a hydrodynamically developed flow to be taken into account

$$Nu_{wv} = 0.0208[1+8.97D(L+12D)]Re_v^{0.8}\,Pr^{1/3}.$$

Heat transfer from a superheated vapour to droplets was calculated according to the well-known empirical relation

$$\alpha_{v\delta} = \frac{\lambda_v}{\delta}\left[2+0.74\left(\frac{S\delta}{\mu_e V_v}\right)^{1/2} Pr^{1/3}\right].$$

A correction to the heat transfer coefficient for flow laminarization by liquid droplets was introduced in the form

$$\alpha_{wv} = \alpha^{\circ}_{wv}(\xi/\xi^{\circ})$$

where α°_{wv}, ξ° are the heat transfer and resistance coefficients calculated without taking into account the effect of droplets.

The value of the resistance coefficient taking into account the effect of droplets, ξ, calculated as a function of the parameter κ using the equation of the universal friction law for smooth tubes is

$$\xi = 8\kappa^2/[\ln(Re\sqrt{\xi}) - \ln(4\sqrt{2\eta_{lam}}) + \kappa\eta_{lam} - 1.5]^2.$$

The quantity ξ is a weak function of the varying dimensionless viscous sublayer thickness η_{lam} and therefore it is assumed that the presence of droplets does not influence η_{lam}.

The constant κ was estimated from the available experimental data as a function of vapour quality.

The hydraulic resistance factors of the vapour flow were determined with the aid of the homogeneous flow model which gives good results for dispersed flows.

In calculations the two-phase flow was assumed to be monodispersed. The choice of the characteristic droplet diameter remains at present to be the most formidable problem in all of the techniques without exception.

In ref. [13] the droplet diameter was determined with the aid of the well-known expression

$$\delta = 1.47D\{\rho_v G x_{lim}[\delta/g(\rho_l - \rho_v)]^{1/2}/\delta\}^{0.675}$$

with the correction factor 1/3. The droplet diameter was also determined using the Weber number. It is assumed that the critical Weber number is equal to 6–8; then the droplet diameter is close to 30–40 μm.

The predicted results were compared with the measured data on the wall temperature for 8 and 12 mm diameter tubes at a pressure of 8 MPa, mass velocities 1400–2000 kg m^{-2} s^{-1} and $q = 2.9\times10^5$–8.7×10^5 W m^{-2}. It is shown that droplets collide with the wall extracting about 15% of heat supplied through the channel wall.

The problems which need further exploration in this model include the determination of the parameter κ and of the size of droplets. That the similarity between the momentum and the heat transfer could be employed, information is also required about the viscous sublayer thickness, rate of droplet deposition and other parameters which were not actually considered under these conditions.

A great deal of attention has been paid to the transient zone of the post dryout heat transfer. Here, a model should be noted which was suggested by Nigmatulin [14] and which analyses in detail the contribution of heat transfer between a hot wall and liquid droplets. It is assumed in the model that the steam is superheated relative to T_s, liquid droplets are at saturation, the slip of phases is taken into account only to determine the heat flux from vapour to droplets, the inertia of droplets is negligible, all the droplets are considered as being the same size, their disintegration and coalescence are ignored.

By numerically solving the general system of equations for a plane-parallel flow the number of droplets reaching the wall, N, is determined, and then the heat flux from the wall to droplets is

$$Q_{w\delta} = q_{w\delta}N.$$

The heat flux $q_{w\delta}$ from the wall to a single droplet is determined from the scheme suggested earlier by Cumo (1969)

$$q_{w\delta} = C\tau_w \pi r_k^2 \lambda_v (T_w - T_s)/\delta.$$

The time of droplet–wall interaction is governed by the natural oscillation of droplets originating due to capillary forces

$$\tau_w \sim (\sqrt{2}/2)\pi\sqrt{[(\rho' r_k^3)/\delta]}.$$

By comparing the model with the experimental data of Bennet for $P = 6.9$ MPa and $\rho w = 350$–5500 kg m^{-2} s^{-1} it was determined that the initial size of droplets corresponded to the critical Weber number of 9. The proportionality factor C is equal to 0 when $\rho w \leqslant 1800$ kg m^{-2} s^{-1}, i.e. the thermal interaction

between droplets and the wall is negligible in this region. When $\rho w \geqslant 1800$ kg m^{-2} s^{-1} the contribution of this interaction begins to increase attaining 30% of the total heat flux, with the vapour–droplet flow tending to thermodynamic equilibrium. The value of C is determined from the following formula:

$$C = 1.5\times10^{-7}\rho w^2 + 1.5\times10^{-4}\rho w - 0.71.$$

A good coincidence was also obtained when comparing the results of the calculation by the model with the experimental data obtained with non-uniform heating along the channel length.

A separate trend is given by the study of the post dryout heat transfer in steam generators heated by liquid metals [15]. In the transient zone, when the vapour quality varies from x_{lim1} (the start of the zone) to x_{lim2} (the end of the transitional zone), there occurs a drastic change in the temperature and heat flux on a heat transfer wall. To determine x_{lim1} for $100 < \rho w < 1000$ kg m^{-2} s^{-1}, the following equation is suggested:

$$x_{\text{lim1}} = 1 - A(p)\rho w + 0.44[A(p)\rho w]^2$$

where

$$A(p)\begin{cases}6.7\times10^{-2}(\rho''/\rho')^{1.8}, & 7.8 \leqslant P \leqslant 11.8 \text{ MPa}\\ 1.14\times10^{-3}, & 11.8 \leqslant P \leqslant 15.7 \text{ MPa.}\end{cases}$$

To determine x_{lim2}, the following equation is used:

$$x_{\text{lim2}} = x_{\text{lim1}} + 0.283D(q_{\text{cr1}} + q_{\text{cr2}})/(rG)$$

where q_{cr1} and q_{cr2} are the specific heat fluxes at the boundaries of the zone of transition from developed boiling to the post dryout region. To determine the statistically-mean heat flux density on the wall in the transient zone, the following equation is suggested:

$$q_{\text{w}} = [\alpha'\omega + \alpha''(1-\omega)](T_{\text{w}} - T_{\text{s}})$$

where α' is the heat transfer coefficient for developed boiling, α'' the coefficient of heat transfer to vapour, and ω the mean fraction of the surface which contacts liquid.

The post dryout heat transfer was calculated on the basis of a many-group heat transfer model under the following assumptions: droplet size distribution at the beginning of the post dryout region is described by the probability density function of Nukiyama–Tanasawa; the vapour temperature and velocity in the given section are equal to their average values; the temperature of the vapour and droplets at the beginning of the post dryout zone is equal to the saturation temperature; there is no deposition of droplets onto the wall when $\rho w < 700$ kg m^{-2} s^{-1} in the case of the second-kind crisis; the discrete spectrum of droplets is used.

The heat fluxes from the wall to the vapour and from the vapour to droplets were calculated from familiar empirical relations.

The system of equations for flow, heat conduction of a wall and energy for liquid sodium were solved numerically on a computer. Comparison of the predicted sodium temperature along the length of the steam generator model with the experimental data shows a good coincidence of prediction with experiment.

The computational models are rather cumbersome and need to be further refined and developed. In view of this, of interest are recommendations for practical calculations of heat transfer in the post dryout region of a vapour–droplet flow taking into account the newly obtained information on experimental results and computational techniques [16, 17].

In ref. [17] it is suggested that the post dryout heat transfer for $\rho w > 1000$ kg m^{-2} s^{-1} and $P = 4$–22 MPa be calculated from the well-known relations suggested by Miropolsky and Groeneweld. When $\rho w < 1000$ kg m^{-2} s^{-1} the calculation should be performed taking into account the thermodynamic non-equilibrium state of the flow. The mean temperature of the superheated vapour is determined in this case as

$$\bar{T}_{\text{v}} = T_{\text{s}} + A(p)[(x_{\text{e}} - x_{\text{a}})/x_{\text{a}}]^{4/3}. \tag{2}$$

The heat transfer coefficient is related to the temperature difference $T_{\text{w}} - \bar{T}_{\text{v}}$ and

$$T_{\text{w}} = \bar{T}_{\text{v}} + \frac{q}{\alpha_{\text{v}}}. \tag{3}$$

The actual vapour quality is determined for tubes from

$$\frac{\mathrm{d}x_{\text{a}}}{\mathrm{d}x_{\text{e}}} = c_1 A(p)\lambda''\frac{\rho''}{\rho'}D\frac{(\rho w)^2}{q}x^2\frac{1-x_{\text{a}}}{x_{\text{a}}}\left(\frac{x_{\text{e}}-x_{\text{a}}}{x_{\text{a}}}\right)^{4/3}$$

where $A(p) = 5\times10^3/P^2 - 43P + 880$; P is given in MPa; q is given in kW m^{-2}; $C_1 = 175$.

The heat transfer coefficient α_{v} in equation (3) is determined from

$$Nu_{\text{v}} = 0.028Re^{0.8}Pr^{0.4}\left(\frac{\rho w}{\rho_{\text{v}}}\right)^{1.15}.$$

Here all the thermophysical properties of the vapour are selected at the average temperature of the superheated vapour $\bar{T}_{\text{v}}$. The recommended technique for calculation was checked at $\rho w = 100$–1000 kg m^{-2} s^{-1}, $q = 0$–0.6 MW m^{-2}; $P = 7$–18 MPa [3, 16]. Figure 4 compares the predicted and experimental results of ref. [3].

It is recommended that the mean heat transfer of a bundle of rods in the post-dryout regime be calculated from

$$\overline{Nu} = Nu''K$$

where Nu'' is found from Miropolsky or Groeneweld's equation; K is the ratio of the mean heat transfer coefficient in the bundle to the heat transfer coefficient in a tube.

The quantity K can be found from the following simple expression:

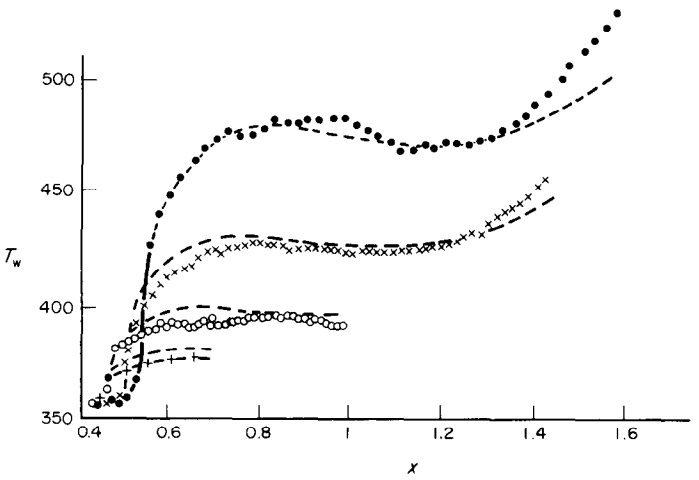

FIG. 4. Comparison of the experimental data from ref. [3] with the results of the calculation technique of ref. [17] at $P = 17.7$ MPa, $\rho w = 550$ kg m^{-2} s^{-1} for a 15×10 mm diameter, 10 m long tube with the heat flux in the 3.8 m long pre-inserted section of 490 kW m^{-2}. The heat fluxes in the 6.2 m long test section are: +, 55.8 kW m^{-2}; ○, 99.8 kW m^{-2}; ×, 158.5 kW m^{-2}; ●, 252.2 kW m^{-2}; ——, prediction.

$$K = 1.1\frac{S}{D} - 0.26$$

where S/D is the relative pitch of the rod bundle.

The minimum heat transfer coefficient in a rod bundle is determined from

$$Nu_{\min} = \overline{Nu}\, j$$

where

$$j = 0.3 + 0.8\left(\frac{S}{D} - 1\right)^{0.25}.$$

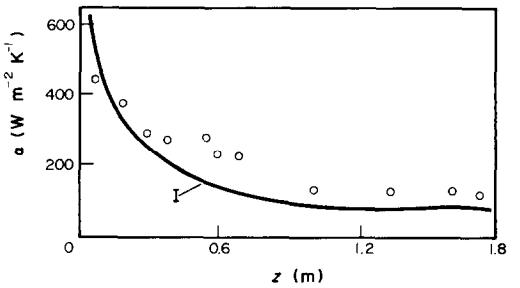

FIG. 5. Variation of the heat transfer coefficient over the non-wetted zone length [18]: $P = 0.5$ MPa; $\rho w = 180$ kg m^{-2} s^{-1}; $T_{en} = 66$°C; $q = 100$ kW m^{-2}; ○, experiment; I, calculation by equation (7) from ref. [2].

4. HEAT TRANSFER ON WETTING HEATED SURFACES

The acquisition of experimental data for both single channels and bundles of rods continued. Experiments were conducted on a single channel (Fig. 1) with both steady-state post dryout heat transfer and conditions of wetting from below. The wetting experiments were carried out in the following parameter ranges: $P = 0.1$–1.1 MPa, $\rho w = 180$–330 kg m^{-2} s^{-1}, $\Delta T_{sub}^{en} = 20$–160°C, $T_w^{in} = 400$–800°C [18, 19].

The data processing was made with the aid of the earlier mentioned information measuring complex (IMC). The heat transfer coefficient was calculated with respect to the temperature difference $\Delta T_w(\tau) = T_w(\tau) - T_s(\tau)$. Figure 5 presents the comparison of the typical experimental values of α with those calculated by the empirical formula from ref. [2] relative to the distance from the wetting front z. It is seen from the figure that the empirical formula qualitatively describes the change of α in a non-wetted zone well, with the experimental values of α generally lying somewhat above the predicted ones, thus allowing this formula to be recommended for reliable practical applications.

Nevertheless, further acquisition of vast experimental information for channels of different geometries and, mainly of larger length, is required. Only then will it be possible to obtain the picture of the interchange of different flow modes in a non-wetted region, ranging from the reversed circular and reversed slug flow to modifications of the dispersed regime with droplets of different size. In the latter case it is possible to expect that an increase of x will be accompanied by an increase of α calculated relative to $\Delta T_w = T_w - T_s$. At present the least studied problems are heat transfer in a non-wetted zone at reduced values of $x_e = (-0.2)-(0.2)$ and the condition of transition to a non-equilibrium dispersed flow the heat transfer to which can be described with the aid of developed techniques of calculation for the steady-state post dryout heat transfer.

In ref. [19], one of the first formulae is given for the post dryout heat transfer in the region of low mass vapour qualities at sufficiently high pressures of 3.5–7 MPa.

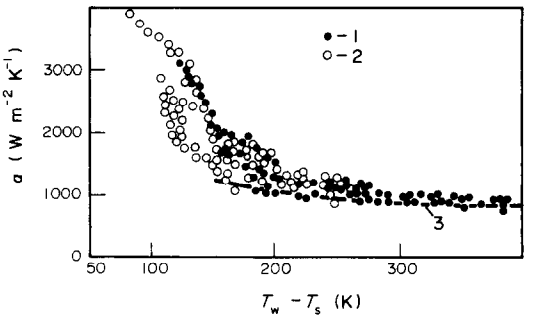

FIG. 6. Variation of the heat transfer coefficient for $\Delta T_w = T_w - T_s$ [19]. $P = 7$ MPa; $\rho w = 700$ kg m^{-2} s^{-1}. 1, Circular channel; 2, semi-rod array; 3, calculation by equation (4).

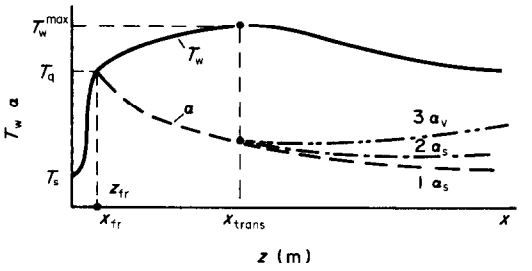

FIG. 7. Variation of the wall temperature and of the heat transfer coefficient with mass vapour quality in a non-wetted zone in long tubes ($L \geq 3.5$ m) for $x_{tran} \geq 0.2$. 1, Calculation of α_s by equation (7) from ref. [2]; 2, 3, the values of α_s, α_v calculated by equations (5) and (6).

The formula obtained on the basis of experimental data has the form

$$\alpha = 1525\lambda'' \left(\frac{\rho w D}{\mu''}\right)^{0.2} Pr_{v,w}^{3}. \quad (4)$$

Here, α (W m^{-2} K^{-1}) is the heat transfer coefficient defined as the ratio of q to $\Delta T = T_w - T_l$; T_l is the temperature of the heat transfer agent. The formula is obtained for $\rho w = 400$–2100 kg m^{-2} s^{-1}, $x_e = (-0.07)-(0.1)$; $q = 0.2$–0.8 MW m^{-2} in a circular and semi-rod channel. The heat transfer coefficient in a tube without spacing elements is below that predicted by equation (4) by about 100 W m^{-2} K^{-1}.

Figure 6 presents the experimental data and the results of the calculation from equation (4). It is seen that α decreases rapidly with an increase of the wall temperature (in the transitional region of boiling), and then depends weakly on it (in the region of stable film boiling).

According to ref. [19], a substantial effect on α is exerted by the conditions of heat transfer agent flow. In the case of reversed slug (plug) flow, the heat transfer coefficient is noticeably smaller (by about a factor of two) than in dispersed flow due to a smaller interphase heat transfer surface. As a result, due to the instability of the boundaries of flow conditions, the heat transfer can differ markedly at virtually the same operational and geometric parameters. Therefore, as yet it is advisable that for such conditions of the post dryout heat transfer computational formulae be constructed that would describe experimental data based on their minimum values.

Reference [10] presents an analysis of the processes of heat removal in the post dryout region and on wetting heating surfaces. In real conditions the wetting of heated surfaces usually occurs when water is supplied to the entrance with $x_e \leq 0$. Because of this, the post dryout heat transfer zone starts at xs much smaller than in the conditions of steady-state post dryout heat transfer. Moreover, the transition heat transfer zone can be more extended due to the rearrangement of the flow structure. It should also be borne in mind here that local flow parameters vary continuously with the motion of the wetting front. Thus, to reliably calculate the heat transfer in a non-wetted zone, one should know the means of calculation of the wetting rate and of the flow parameters in it. Moreover, one should take into account the initial period of cooling which can be rather long at small velocities of water entry into long channels.

To calculate heat transfer in the conditions of wetting, the sequence of all the stages of such a process is considered for the main means of water supply—flooding from below. When water enters a dried channel, the steam generation starts virtually instantaneously, but a definite time is needed for the entire channel to be filled up with a steam–water mixture because of the entrainment of liquid by steam. The conditions of liquid jet fragmentation can be determined with the aid of the criterion suggested by Arrietta and Yadigaroglu in 1978 [20], while the entrainment of droplets can be determined from formulae suggested in ref. [21].

The heat transfer in the non-wetted zone with water supply from below is governed by the flow parameters and wall temperature. Consider the heat transfer after the onset of the entrainment phenomenon when the entire channel is filled up with a steam–water mixture with the rate close to that at the entrance.

Within the region with $\Delta T_w > T_q - T_s$ there are usually two zones separated by the value T_w^{max} (Fig. 7). The first zone represents the transitional region, where, according to refs. [5, 10], the development and stabilization of the thermal boundary layer occurs under the conditions of varying flow structure. In the conditions of wetting of the heating surface the second zone can be considered as an analogue of the corresponding post dryout heat transfer zone in steady-state conditions.

In the region with $\Delta T_w > T_w - T_s$, different regimes of flow may exist depending on x and ρw. However, at small ρw and relatively high q, with $T_w \gtrsim 500$°C at the beginning, the conditions for the formation of the dispersed flow structure, at least in the second zone of the non-wetted region, are rather quickly attained.

Experimental and computational investigations of the modes of post dryout heat transfer in steady-state conditions have shown that a dispersed flow is

substantially in nonequilibrium from the thermodynamic viewpoint. To calculate x_a, a number of formulae and calculation techniques have been suggested which are given above. However, at small values of x_e and x_a, occurring during wetting of heated surfaces, these formulae do not apply. To approximately calculate x_a, a simplified formula can be used [22] which has the form

$$x_a = 1-(1-x_{cr})\exp(x_{cr}-x_e) \quad (5)$$

provided $x_{cr} = x_{fr}$.

Comparison of equation (5) with the equations for steady-state post dryout heat transfer shows that at least up to $x_{cr} < x_e \leqslant 1$ there is a good agreement.

The use of equation (5) for the determination of T_v shows that there is rather a satisfactory agreement with separate available values of T_v at x_e (at the entrance to the channel) equal to 0.08–0.27 and at x_e (at the point of measurement) equal to 0.2–0.4.

Thus, there appears the possibility to describe a portion of the heat transfer zone in the non-wetted region with the aid of relations obtained for the steady-state post dryout heat transfer [10]

$$\alpha_v = 0.0246\frac{\lambda_v}{D}\left(\frac{\rho w D}{\mu_v}\right)^{0.8} \times\left[\left(x_a+\frac{\rho_v}{\rho'}\right)(1-x_a)\right]^{0.8} Pr_w^{0.8}. \quad (6)$$

For the data obtained when $x_e > 0.2$ and far from the wetting front, there is rather a satisfactory agreement between prediction and experiment.

It should be noted that when $x_e > 0.2$ the quantity α_s related to $\Delta T_w = T_w - T_s$, but calculated from equation (6), can increase with x_e (Fig. 7). At the same time, over rather an extended portion of the non-wetted zone adjacent to the wetting front, a decrease in α_s is observed. Thus, earlier in ref. [2] the following formula was suggested:

$$\alpha_s = \frac{(a_1+a_2P)(\rho w)^{a_3}}{1+a_4z+a_5z^2}\ \mathrm{W\,m^{-2}\,K^{-1}} \quad (7)$$

where a_1, a_2, a_3, a_4, a_5 are constants and $0.01 \leqslant z \leqslant 2.5$ m. A further comparison of equation (7) with experimental data shows that equation (7) underestimates the results on heat transfer when $z >$ 0.5–0.7 m. This can be attributed to the fact that, due to the complexity in the choice of the data when processing their large files, the points which had been obtained before the start of liquid entrainment were not separated, i.e. in the transitional period when α increases practically from zero up to a more or less stable value.

Based on equation (7) the following formula was obtained in ref. [23] to estimate the minimum value of α_s in a non-wetted zone at the conditions when the entire channel is filled up with a steam–water mixture:

$$\alpha_s = 5.85P^{0.26}\rho w^{0.56}\ \mathrm{W\,m^{-2}\,K^{-1}}.$$

This formula is valid at $P = 0.1$–0.5 MPa, $\rho w = 25$–$250\ \mathrm{kg\,m^{-2}\,s^{-1}}$.

In a general case use of equation (7) is recommended for the transitional zone adjacent to the wetting front and, on attaining $x_e^a > 0.2$ and $Re_v > 10^4$, use of equation (6) with x_a calculated from equation (5). When $Re_v < 10^4$, for tubular smooth channels it is possible to use the laminar heat transfer model suggested in ref. [24].

5. CONCLUSION

In the works considered the next step in the study of post dryout heat transfer and on wetting heated surfaces has been made. Certain successes are attained in the refinement of heat transfer models in a dispersed mist flow under steady-state conditions. Further investigations are required of the structure of flow and post dryout heat transfer modes under the conditions of the wetting of channels in a wide range of mass vapour qualities and also of the effect of spacing grids in bundles of rods on these processes.

REFERENCES

1. N. Rassokhin, Emergency cooling heat transfer problem of nuclear reactors. In *Heat Transfer Nuclear Reactor Safety Seminar* (Dubrovnik, 1–5 September 1980), pp. 203–222. Washington (1982).
2. N. G. Rassokhin, L. P. Kabanov, V. M. Mordashev, S. P. Nikonov and R. K. Khasanov, Rewet heat transfer in hot tubes cooled by bottom, top flooding and cooling films. In *Heat Transfer Nuclear Reactor Safety Seminar* (Dubrovnik, 1–5 September 1980), pp. 797–808. Washington (1982).
3. P. L. Kirillov, B. V. Kokorev, O. V. Remizov and V. V. Sergeyev, Post-dryout heat transfer. In *Proceeding of the 7th Int. Heat Transfer Conference* (München), paper NR 16, pp. 487–492 (1982).
4. L. P. Kabanov, Der Wärmeübergang der Wiederbenetzung der Heizflachelung von Druckwasserreaktoren, *Kernenergie* **24**(7), 253–257 (1981).
5. M. A. Styrikovich, V. S. Polonsky and G. V. Tsiklauri, *Heat Transfer and Hydrodynamics in Two-phase Flows of Nuclear Power Plants*. Izd. Nauka, Moscow (1982).
6. V. E. Doroshchuk, *Dryout Heat Transfer During Water Boiling in Tubes*. Energoatomizdat, Moscow (1983).
7. E. F. Galchenko and V. V. Sergeyev, Toward the generalization of data on limiting vapour contents, *Teploenergetika* No. 3, 58–59 (1983).
8. O. K. Smirnov and V. K. Afonin, The effect of the heat flux density on the critical vapour content at small mass velocities of a steam–water mixture, *Teploenergetika* No. 6, 38–41 (1984).
9. G. V. Tsiklauri and T. S. Dzhishkariani, Investigation of the non-equilibrium state of a mist flow in the post-dryout region at small mass velocities and low pressure, *Teplofiz. Vysok. Temp.* **21**(1), 130–136 (1983).
10. L. P. Kabanov, Heat transfer on reflooding of the active zone of pressurized water reactors. In *The Problems of Nuclear Science and Technology. Physics and Technology of Nuclear Reactors*, No. 7(36), pp. 41–49 (1983).
11. M. N. Burdunin, Yu. A. Zvonaryov, A. S. Komendantov and Yu. A. Kuzma-Kichta, Investigation of the post dryout heat transfer in a channel of complex geometry. In *Heat and Mass Transfer-84*, Vol. IV, pp. 41–46 (1984).

12. O. V. Remizov, V. V. Sergeyev and Yu. I. Yurkov, An experimental investigation of deteriorated heat transfer in ascending and descending water flow in a tube, *Teploenergetika* No. 9, 64–66 (1983).
13. M. A. Styrikovich, Yu. V. Baryshev, M. E. Grigorieva and E. M. Konovalova, A model for the calculation of heat transfer for a steam–water dispersed flow, *Teplofiz. Vysok. Temp.* **21**(1), 122 129 (1983).
14. B. I. Nigmatulin, Post-burnout dispersed steam–droplet flow in heated channels. In *Two-phase Annular and Dispersed Flows* (an International Symposium held at the University of Pisa, Italy, 24–29 June 1984), Abstracts, ETS Pisa, pp. D 3, 1-D 3, 4.
15. V. G. Bazhin, N. S. Grachyov, D. Yu. Kardash and V. V. Khudasko, Concerning the calculation of post dryout heat transfer region of a steam generating channel with sodium heating. Preprint of the Physical-Power Engineering Institute No. 1496, Obninsk (1983).
16. E. F. Galchenko, V. V. Sergeyev, Yu. N. Yurkov and O. V. Remizov, Investigation of heat transfer deterioration in circular channels, *Teploenergetika* No. 10, 44–46 (1984).
17. P. L. Kirillov, Yu. S. Yuriev and V. P. Bobkov, *Handbook of Thermal and Hydraulic Calculations*. Energoatomizdat, Moscow (1984).
18. Yu. A. Zvonarev, A. S. Komendantov and Yu. A. Kuzma-Kichta, An experimental investigation of the heat transfer characteristics in the case of repeated wetting of the heating surface, *Teploenergetika* No. 5, 64–66 (1984).
19. V. P. Volkov, A. Ya. Kramerov and G. I. Savvatimsky, Features of transient following loss-of-coolant accidents and emergency core cooling systems in pressure-tube boiling water reactors. In *Experimental and Modelling Aspects of Small-break LOCA. Proceedings of a Specialist's Meeting*, IAEA, Budapest, Hungary, 3–7 October, pp. 134–143 (1983).
20. J. M. Delhaye, M. Giot and M. L. Rietmuller (Editors), *Thermohydraulics of Two-phase Systems for Industrial Design and Nuclear Engineering*. Hemisphere, Washington, DC (1981).
21. S. S. Kutateladze and M. A. Styrikovich, *Hydrodynamics of Gas–Liquid Systems*. Izd. Energiya, Moscow (1976).
22. G. Barzoni and R. Martini, Post dryout heat transfer: an experimental study in a vertical tube and a simple theoretical method for predicting thermal non-equilibrium. In *Proceedings of the 7th Int. Heat Transfer Conference* (München), pp. 411–416 (1982).
23. L. P. Kavanov, The efficiency of the emergency cooling of power plant reactors with water coolant, *Teploenergetika* No. 2, 4–10 (1983).
24. S. Yao and K. H. Sun, A dispersed flow heat transfer model for flow bottom reflooding conditions. In *Heat Transfer Nuclear Reactor Safety Seminar* (Dubrovnik, 1–5 September 1980), pp. 763–776, Washington (1982).

TRANSFERT THERMIQUE DANS LA REGION APRES ASSECHEMENT ET SUR LES SURFACES CHAUDES REMOUILLEES

Résumé—On donne une revue des travaux publiés en Union Soviétique en 1983 et 1984, sur le transfert thermique dans la région après assèchement et sur les surfaces chaudes remouillées. Des nouvelles données expérimentales, des modèles de transfert thermique et des techniques de calcul sont analysés. On note les complexités des mécanismes de transfert de chaleur dans ces conditions. On indique les differences et les aspects communs des mécanismes de transfert thermiques dans la région après assèchement et sur les surfaces remouillées, ainsi que la nécessité du développement des techniques de calcul qui doivent considérer simultanément les deux mécanismes.

WÄRMEÜBERGANG IM POST-DRYOUT-GEBIET UND AN BENETZENDEN BEHEIZTEN OBERFLÄCHEN

Zusammenfassung—Es wird ein Überblick über die in der Sowjetunion in den Jahren 1983 und 1984 veröffentlichten Arbeiten zum Wärmeübergang im Post-Dryout-Gebiet und an benetzenden beheizten Oberflächen gegeben. Neue Meßwerte, Wärmeübergangsmodelle und Berechnungsmethoden werden untersucht. Die Komplexität des Wärmeübertragungsprozesses unter den oben genannten Bedingungen wird dargestellt. Es werden sowohl die Unterschiede und Gemeinsamkeiten der Wärmeübertragungsprozesse im Post-Dryout-Gebiet und an benetzenden beheizten Oberflächen aufgezeigt als auch die Notwendigkeit zur Entwicklung eines Berechnungsverfahrens, welches diese beiden Prozesse gleichzeitig beinhaltet.

ТЕПЛООТДАЧА В ЗАКРИЗИСНОЙ ОБЛАСТИ И ПРИ СМАЧИВАНИИ РАЗОГРЕТЫХ ПОВЕРХНОСТЕЙ

Аннотация—Приведен обзор работ, опубликованных в Советском Союзе в 1983–84 гг., по теплоотдаче в закризисной области и при смачивании разогретых поверхностей. Анализируются новые экспериментальные данные, модели теплоотдачи, методики расчета. Отмечаются сложности процесса теплоотдачи в рассматриваемых условиях. Указано на отличия и общие черты процессов теплоотдачи в закризисной области и при смачивании разогретых поверхностей и на целесообразность разработки методик расчета, рассматривающих оба процесса совместно.